ACS APPLIED MATERIALS & INTERFACES

Research Article

www.acsami.org

Fabrication and Characterization of Thermoplastic Elastomer Dry Adhesives with High Strength and Low Contamination

Walid Bin Khaled* and Dan Sameoto

Department of Mechanical Engineering, University of Alberta, 4-9 Mechanical Engineering Building, Edmonton, Alberta T6G 2G8, Canada

ABSTRACT: Polydimethylsiloxane (PDMS) and polyurethane elastomers have commonly been used to manufacture mushroom shaped gecko-inspired dry adhesives with high normal adhesion strength. However, the thermosetting nature of these two materials severely limits the commercial viability of their manufacturing due to long curing times and high material costs. In this work, we introduce poly(styrene-ethylene/butylene-styrene) (SEBS) thermoplastic elastomers as an alternative for the manufacture of mushroom shaped dry adhesives with both directional and nondirectional performance. These materials are attractive for their potential to be less contaminating via oligomer transfer than thermoset elastomers, as well as being more suited to mass manufacturing. Low material transfer properties are attractive for adhesives that could potentially be used in cleanroom environments for microscale assembly and handling in which device contamination is a serious concern. We characterized a thermoplastic elastomer in terms of oligomer transfer using X-ray photoelectron spectroscopy and found that the SEBS transfers negligible amounts of its own oligomers, during contact with a gold-coated silicon surface, which may be representative of the metallic bond pads found in micro-electro-mechanical systems devices. We also demonstrate the fabrication of mushroom shaped isotropic and anisotropic adhesive fibers with two different SEBS elastomer grades using thermocompression molding and characterize the adhesives in terms of their shear-enhanced normal adhesion strength. The overall adhesion of one of the thermoplastic elastomer adhesives was found to be stronger or comparable to their polyurethane counterparts with identical dimensions.

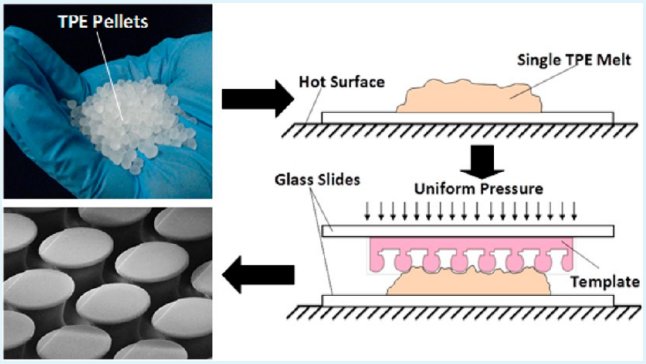

KEYWORDS: *dry adhesive, gecko, van der Waals, thermoplastic elastomer, oligomer, anisotropic*

1. INTRODUCTION

The remarkable ability of geckos to climb up and down on almost any surface at any orientation, including inverted ones, at speeds of over 1m/s has amazed researchers for centuries. After the discovery by Autumn et al. that van der Waals interactions are the primary mechanism for generating gecko adhesion[1] and the subsequent understanding of gecko adhesion mechanism in detail,[2−5] a great deal of effort has been spent attempting to synthetically reproduce gecko-like adhesion by fabricating micro- and/or nanoscale polymer fibers.[6] A common way to fabricate these adhesives is to create a positive or negative template by photolithography followed by subsequent casting with prepolymers such as PDMS and/or polyurethane on the template/mold to make the final adhesives.[7−11] Even though thermosetting polymers such as PDMS and polyurethane have been proven to be useful materials for microstructured adhesives, they have limitations such as long processing times due to their curing reactions, frequent requirement of vacuum for degassing the prepolymers, and relatively high base material costs, all of which renders soft lithography techniques with thermosetting polymers challenging for large-scale production of dry adhesives. We introduce thermoplastic elastomer SEBS polymers as an alternative to the thermosetting PDMS and polyurethane for manufacture of dry adhesives and characterize the thermoplastic elastomer in terms of oligomer transfer and adhesion strength.

In certain applications of dry adhesives such as micro-electro-mechanical systems (MEMS) pick and place[12] and micro-transfer printing,[13−15] the issue of surface contamination by oligomer transfer is of high importance as it might impede the normal operation of the device being handled. For our targetted application of MEMS die pick and place after wafer dicing, a strong normal adhesive strength is desireable to remove die from tape drums or gel paks without needing a suction tip (potentially permitting all assembly and packaging to be done in an ultra clean vacuum). For this reason, a fiber design with overhanging caps is needed, and the dry adhesive structural material should have the mimimal contamination of material like gold, which would subsequently be wire bonded. Careful analysis of surface contamination is therefore necessary before choosing a material for dry adhesives to be applied in those applications. It is already well established through various

Received: January 28, 2014
Accepted: April 8, 2014
Published: April 8, 2014

experiments on microcontact printing that PDMS transfers oligomers,[16−26] but little information is available, if any, on the oligomer transfer from polyurethane or thermoplastic stamps. Trimbach et al. claimed in their article[27] that unlike PDMS, Kraton SEBS does not transfer oligomers during microcontact printing, but they did not present any experimental evidence to back their claim. This conclusion may be feasible, however, because unlike a cross-linkable material, SEBS is already supplied as a relatively high molecular weight polymer that is held together through secondary bonds rather than covalent bonds. The high molecular weight should reduce the tendency of the molecules to move around or be easily separated from the surface. Oligomers are small fragments of cross-linkable monomers that are not successfully bonded into the complete polymer matrix and can therefore diffuse through the material and to the surface where transfer can more readily occur. Transfer of oligomers due to contact is thought to take place because of molecular interactions, electrostatic forces, etc.[28] and can depend on factors such as contact time,[29,18] contact pressure, curing and or pretreatment of the stamp, surface energy,[17] etc. Previous studies to investigate the surface contamination from contact used processes/tools like X-ray photoelectron spectroscopy (XPS),[21,23,30,16] infrared reflection-absorption spectroscopy (IRAS)[22] time-of-flight secondary ion mass spectroscopy (ToF-SIMS),[31,20] Fourier transform spectroscopy (FT-IR),[30,16] atomic force microscopy (AFM),[32,29,16] optical micrographs,[33] and scanning electron microscopy (SEM).[33] In this work, we investigate oligomer transfer from polyurethane, PDMS, and an SEBS thermoplastic elastomer from contact with a rigid surface using high resolution X-ray photoelectron spectroscopy (XPS). We chose this method over alternatives such as contact angle measurements due to its relatively good abilities at distinguishing the composition of adsorbed elements for transferred materials. Specifically, this method permitted detection of any transfer of PDMS oligomers via an intermediate means (polyurethane or Kraton in this case). This secondary PDMS transfer is a potential area of concern with any molding approach that uses a negative silicone rubber template.

Figure 1 shows the molecular structure of these three polymer materials. Presence of any material on a surface is usually confirmed by detecting photoelectrons from any element, preferably unique, from the material being investigated and/or comparing the amount of photoelectron with a control sample. For this investigation, Si 2s electrons were used to detect PDMS oligomers (Figure 1b), N 1s electrons to detect polyurethane oligomers (Figure 1a), and C 1s to detect Kraton SEBS oligomers (Figure 1c).

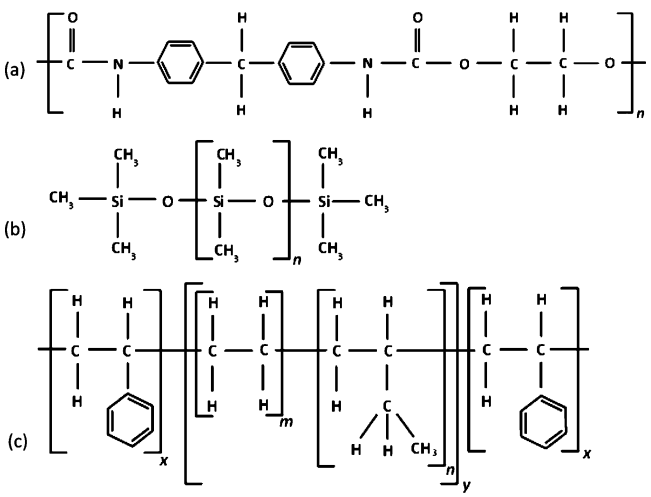

Figure 1. Molecular structures of (a) polyurethane, (b) PDMS, and (c) Poly(styrene-ethylene/butylene-styrene) (SEBS).

In the second part of this work, we show how mushroom shaped dry adhesives can be fabricated from thermoplastic elastomers using a thermocompression molding technique. Previous reports on thermoplastic dry adhesives includes fabrication of adhesive fibers from thermosensitive shape memory polymers.[34] The fibers switched from an inclined state to vertical state when heated above the glass transition temperature, resulting in a 200-fold increase in adhesion forces. Majidi et al. fabricated an array of microfibers from stiff thermoplastic polypropylene.[35] The fibers, despite showing high friction, had negligible normal adhesion and further developments with this particular fabrication technology[36] continued to use nearly cylindrical fibers without specific cap shapes. To the best of our knowledge, there is no report on fabrication of mushroom shaped fibers, which is thought to be the optimum fiber shape to achieve high adhesion,[37,38] with materials other than thermoset rubbers like polyurethanes and PDMS. In this work, isotropic and anisotropic adhesives were fabricated from two versions of SEBS thermoplastic elastomers with slightly different material properties, and their adhesion strength was compared with a polyurethane version of the same adhesives.

2. SURFACE ANALYSIS USING X-RAY PHOTOELECTRON SPECTROSCOPY (XPS)

2.1. Sample Preparation. SEBS and polyurethane pucks were made by casting on separate silanized borofloat glass substrates as well as on separate plain PDMS surfaces followed by curing or drying, mimicking a common practice of casting a polymer on a negative PDMS template to produce micro-structured adhesive fibers. The PDMS pucks were produced by casting on two separate silanized borofloat glass substrate followed by degassing and curing at 80 °C in an oven for 2 h. A few circular dots of PDMS were also produced in a separate section of one of the substrates.

An SEBS solution was previously prepared by adding 5 g of solid Kraton G1657 pellets (Kraton Performance Polymers Inc.) to 75 mL of hexane followed by stirring with a magnetic stirrer. The SEBS solution was cast multiple times on the PDMS surface, in the form of arrays of dots(~10 mm diameter), to produce a layer of a few hundred micrometers thick after the hexane evaporated. This eliminated the majority of the dust that would otherwise be present on the pellets of neat resin and was otherwise not feasible to remove. The polyurethane puck was made of ST-1060 (BJB Enterprises), a thermoset elastomer commonly used to produce dry adhesives,[10,39−41] which was prepared by mixing the two components to the manufacturers recommended ratio followed by degassing, and casting on the second PDMS puck, also in the form of arrays of dots, followed by curing at room temperature for at least 48 h.

Several gold-coated silicon dies were cleaned by dipping into a piranha solution (3 part H_2SO_4 (96%) and 1 part H_2O_2 (30%)) for 15 min followed by rinsing with DI water and drying with nitrogen. ***Caution!*** piranha solution is aggressive and explosive. Never mix piranha waste with solvents. Check the safety precautions before using it. The PDMS, polyur-

dx.doi.org/10.1021/am500616a | ACS Appl. Mater. Interfaces 2014, 6, 6806−6815

ethane, and SEBS pucks were then brought separately into contact with the surface of gold-coated silicon dies for durations of 5, 15, and 60 s as outlined in Table 1. All the samples were prepared within 1 h of the cleaning in a cleanroom environment and left sealed in containers before mounting on the XPS stage. For applications like MEMS pick-and-place, these adhesives would be expected to be in contact for relatively short times and therefore these contact periods were felt to be representative of our expected applications.

Table 1. Material, Conditions and Durations of Contact of the Polymer Pucks with the Dies

	sample no.	contact material/condition	contact time (s)
	1	control wafer (no contact)	0
Case 1	2	plain polyurethane	5
	3	plain polyurethane	15
	4	plain polyurethane	60
Case 2	5	polyurethane cast on PDMS	5
	6	polyurethane cast on PDMS	15
	7	polyurethane cast on PDMS	60
Case 3	8	plain Kraton G1657	5
	9	plain Kraton G1657	15
	10	plain Kraton G1657	60
Case 4	11	Kraton G1657 cast on PDMS	5
	12	Kraton G1657 cast on PDMS	15
	13	Kraton G1657 cast on PDMS	60
Case 5	14	plain PDMS	5

2.2. XPS Parameters. The XPS measurements were performed on an ULTRA XPS spectrometer (Kratos Analytical) in the Alberta Centre for Surface Engineering and Science (ACSES) at the University of Alberta. The base pressure in the analytical chamber was lower than 3×10^{-8} Pa. Monochromatic Al Kα source ($h\nu$ = 1486.6 eV) was used at a power of 210 W. The analysis spot was 400 × 700 um. The resolution of the instrument is 0.55 eV for Ag 3d and 0.70 eV for Au 4f peaks.

The survey scans were collected for binding energies spanning from 1100 eV to 0 with an analyzer pass energy of 160 eV and a step of 0.4 eV. For the high-resolution spectra, the pass energy was 20 eV with a step of 0.1 eV. Charge neutralization was not required. Vision-2 instrument software was applied to process the data. All spectra were calibrated for C 1s binding energy position at 284.8 eV.

2.3. XPS Results. Preliminary data analysis and atomic compositions were calculated using Casa XPS software. The compositions were calculated using Scofield sensitivity factors. The high resolution XPS spectrum data points were then exported to a spreadsheet and plotted as shown in Figure 2. The elements of interest are carbon (common to all the polymers), oxygen (found in the PDMS and polyurethane), nitrogen (found only in the polyurethane), and silicon (found only in the PDMS). The gold layer was thick enough to not permit any of the underlying silicon wafer from interfering with the measurements.

The binding energies of the relevant photoelectrons are given in Table 2. From Figure 2(a), which compares the N 1s spectra of case 1 samples with that of the control sample, we can see that the peaks at 399 eV for the case 1 samples are a little more pronounced than that corresponding to the control sample, suggesting that the case 1 samples have a higher N 1s content. This is verified by the atomic composition calculation in Table 3, where N 1s concentration was found to have increased slightly from 0.5% in the control sample to 1.6%, 1.3%, and 1.8% in samples 2, 3, and 4, respectively. The decrease of the background Au 4f % from the control sample to the case 1 samples and a simultaneous increase in N 1s content is suggestive of a possible polyurethane oligomer transfer from the puck to the die surface during contact. A similar trend of increase in N 1s concentration and decrease in Au 4f concentration can be observed for Case 2 samples, corroborating our findings above. Interestingly, there is a slight increase in Si 2s concentration for sample 6 and 7 as compared to negligible amount in the control sample, as shown in Table 3, suggesting that some oligomers might have made its way from the PDMS mold to the dies via the polyurethane puck. The slight bulging of the spectrum at 153 eV in Figure 2c for Case 2 samples supports the suggestion. This cross contamination of PDMS from an original mold will also be a possible concern for any adhesives manufactured with soft-lithography techniques, but would potentially be solvable via some surface cleaning of adhesives prior to use. In these measurements, sources of error can include variations in transfer across a single sample and the introduction of operator judgment in measuring the peaks, along with inherent noise within the signal. The composition percentages can generally be considered accurate within 10%.

Regarding the Case 3 SEBS samples, we can see that the O 1s concentration dropped amid a slight increase of C 1s concentration, which suggests that there might be some SEBS oligomer transfer as well, which consists of only carbon and hydrogen. If the original carbon and oxygen content is primarily adsorbed CO_2, then it is possible that some of this is displaced by the SEBS, although the gold concentration remains so close to the original control sample that it is possible that there is negligible transfer. Similar to Figure 2c, the Si 2s peaks for samples 11, 12, and 13 in Figure 2d also shows that some PDMS oligomers might have made its way into the die via the intermediate SEBS puck. The increase in Si 2s atomic concentration for samples 11 and 12 in Table 3 corroborates this observation.

Referring to Figure 2e and atomic composition values in Table 3, we can see that there is an obvious Si 2s peak in the XPS spectra for sample 14. The concentration of Si 2s increased from a negligible amount in the control sample to 3.2% in sample 14, indicating oligomer transfers from PDMS puck to the gold-coated die surface, as are expected without significant modification to the silicone.[19,20]

In all the cases, there is little evidence of significant variation in the amount of material transferred at different contact duration which agrees with previous reports[18,29] where the amount of oligomer transfer increased significantly only at large duration of contact($\gg$1 min) and not within a minute period, which was the range of duration of contact in our work. Given the general levels of composition and adsorbed carbon on even the control sample, it is apparent that the amount of material transferred from Kraton onto the gold surfaces is very small and, if it is in its pure form without any surface contamination from PDMS, appears to have the least rate of transfer of the materials tested. Multiple contacts of Kraton with a clean surface should mostly deplete this supply of surface oligomers and reduce the possibility of transfer with future use. From this, we can conclude that Kraton SEBS would be an acceptable choice as a low or minimally contaminating thermoplastic elastomer candidate in comparison to curable polyurethane or silicone thermoset elastomer.

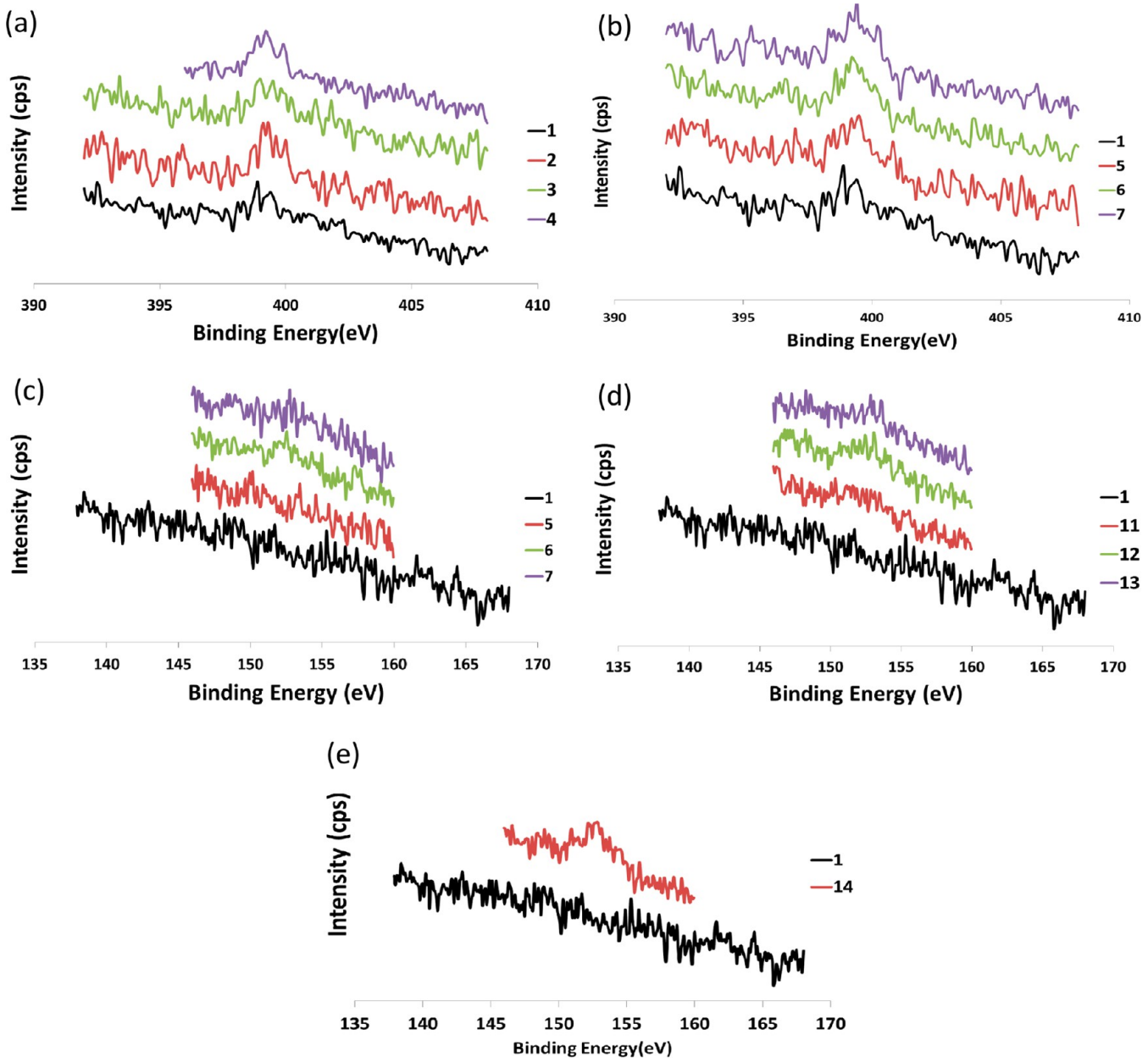

Figure 2. High resolution XPS spectra comparing control sample with (a), (b) Case 1 and 2 samples showing N 1s peaks; (c–e) Case 2, 4, and 5 samples showing Si 2s peaks. Some of the spectra are deliberately offset in the *y*-direction for clarity.

Table 2. Binding Energies and Relative Sensitivity Factors of the Relevant Photoelectrons[42]

photoelectron	binding energy (eV)	relative sensitivity factors
Si 2s	149	0.955
C 1s	284	1.00
N 1s	399	1.8
O 1s	532	2.93
Au 4f 7/2	83	9.58

3. CHARACTERIZATION OF THERMOPLASTIC ELASTOMER ADHESIVES

Although the material transfer of SEBS was found to be very small, it would still not be an acceptable material for use if it did not have comparable adhesion properties (such as adhesion strength, long-term durability and directionality) to those of the thermoset rubbers with identical microstructures. Of great importance to our application is a high normal adhesion strength when pulled directly off of a substrate (to remove MEMS die or devices from tape or substrates) and the ability to demonstrate directional behavior (for easy release) when structured with a particular defect to make them more vulnerable to peeling when loaded with a shear force. The manufacturing and testing of these particular adhesive variations is described below.

3.1. Fabrication. Isotropic and anisotropic adhesive samples were fabricated out of Kraton SEBS by thermocompression molding, shown in Figure 3, and their performance is compared with a polyurethane version manufactured from ST-1060. In this case, another version of Kraton SEBS (G1645) was used that had a lower shore A hardness (~Shore A 35). The softer G1645 was qualitatively stickier than G1657, even in its unstructured form, but it did require more force or time to flow into molds at elevated temperatures, as indicated by the

dx.doi.org/10.1021/am500616a | ACS Appl. Mater. Interfaces 2014, 6, 6806–6815

Table 3. Atomic Composition Calculated from High Resolution Spectrum Shown in Figure 2

		atomic composition (%)				
case	sample	N 1s	C 1s	O 1s	Si 2s	Au 4f
control	1	0.5	23.8	5.2	~0.0	70.5
	2	1.6	23.1	4.6	~0.0	70.7
1	3	1.3	24.8	6.5	~0.0	67.4
	4	1.8	24.0	6.1	~0.1	68.1
	5	2.5	24.1	4.4	0.6	68.4
2	6	1.8	25.6	5.8	2.0	64.8
	7	2.2	24.9	7.1	1.5	64.3
	8	~0.0	25.4	5.0	~0.0	69.6
3	9	0.1	25.0	4.0	~0.0	70.9
	10	~0.0	25.3	2.7	~0.0	71.9
4	11	0.6	25.0	4.7	2.6	67.2
	12	0.7	23.6	5.5	3.0	67.2
	13	0.7	26.8	4.7	1.0	66.8
5	14	0.4	24.9	7.0	3.2	64.5

lower melt-flow rate. Such factors are ultimately necessary to consider in the trade-off between easy manufacturability and final adhesive performance because fibers with undesired defects will be much worse even if structural properties are more attractive. Although other Kraton varieties were tested, not all were sufficiently flow-able at the temperatures and forces used to manufacture the adhesives in this work and are not reported here.

A negative template, made by casting silicone (TC-5030, BJB Enterprises) on a rigid mold in a process described elsewhere,[43] was used as the master here. The template consists of the negative of both isotropic and anisotropic mushroom shaped fibers.

The polyurethane versions of the adhesive fibers were manufactured by mixing ST-1060 polyurethane prepolymer (BJB Enterprises, CA, USA) with the catalyst on a 100:55 ratio and casting on the silicone mold followed by degassing, curing at room temperature for at least 8 h, and postcure baking for another 8 h at 80 °C in an oven. The thermoplastic versions were made by a hot embossing/thermocompression molding process, shown in Figure 3. Kraton G1657 and G1645 were obtained from Kraton Performance Polymers Inc. (TX, USA). The relevant material properties are outlined in Table 4. Some recently reported work[44] suggests that viscoelastic components of material properties strongly influence adhesion behavior if a material is tested at a temperature at close proximity to its glass transition temperature T_g. There is no reported glass transition

Table 4. Select Material Properties of ST-1060 Polyurethane,[47] Kraton G1645,[48] and Kraton G1657[49]

properties	ST-1060	Kraton G1657	Kraton G1645
melt flow at 230 °C (g/10 min)	N/A	22	2–4.5
hardness, Shore A	60	47	35
tensile Strength (psi)	900	3400	1500
elongation at break (%)	590	750	>600
modulus of elasticity at 300% (psi)	560	350	N/A
glass transition temperature	N/A	~−42 °C[49]	N/A

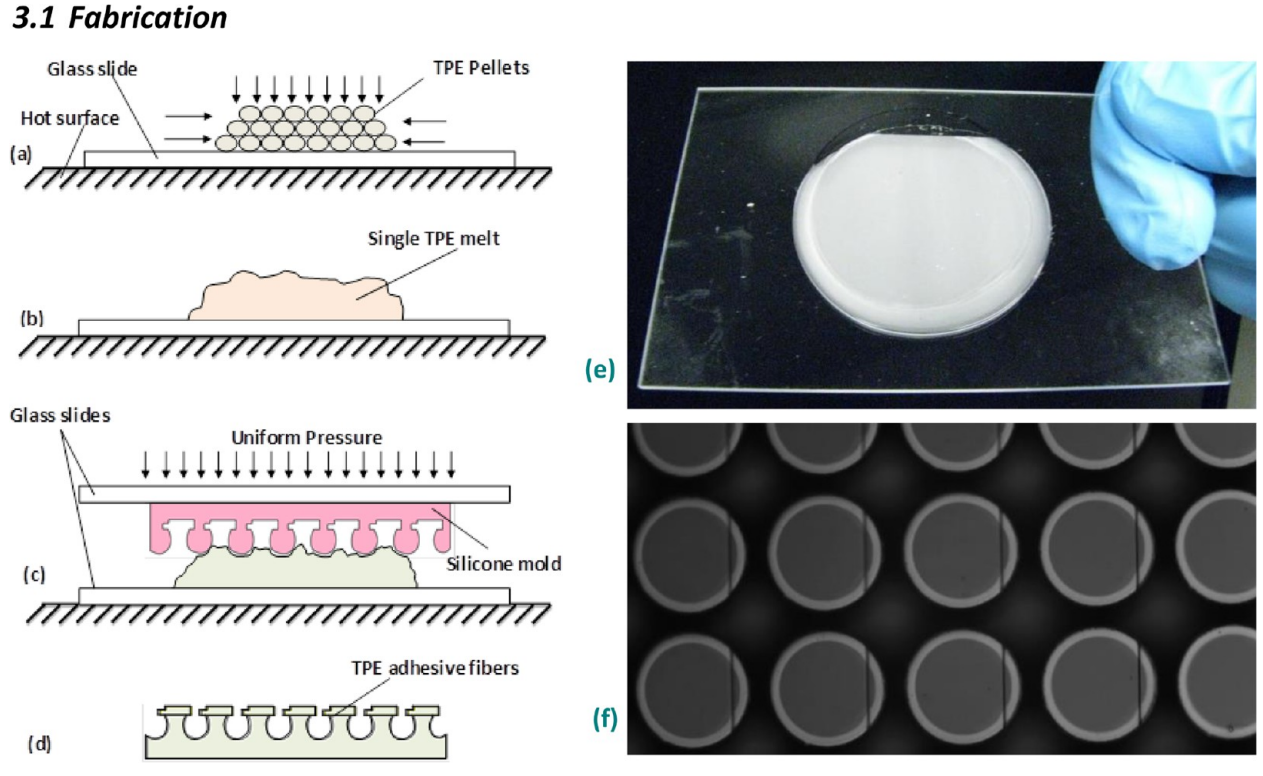

Figure 3. Schematic diagram showing the fabrication of thermoplastic elastomer (TPE) adhesives by thermocompression molding. (a and b) SEBS pellets are melted together under light pressure to form a melt, (c) a silicone rubber mold is placed on the melt a pressed down slowly until the desired force is applied, (d) after approximately 30 s to fill the mold, the silicone, SEBS and glass slide are removed from the hot plate and cooled before the silicone is demolded, (e) macroscale view of an SEBS adhesive sample, and (f) microscopic image showing arrays of anisotropic adhesive fibers made of SEBS.

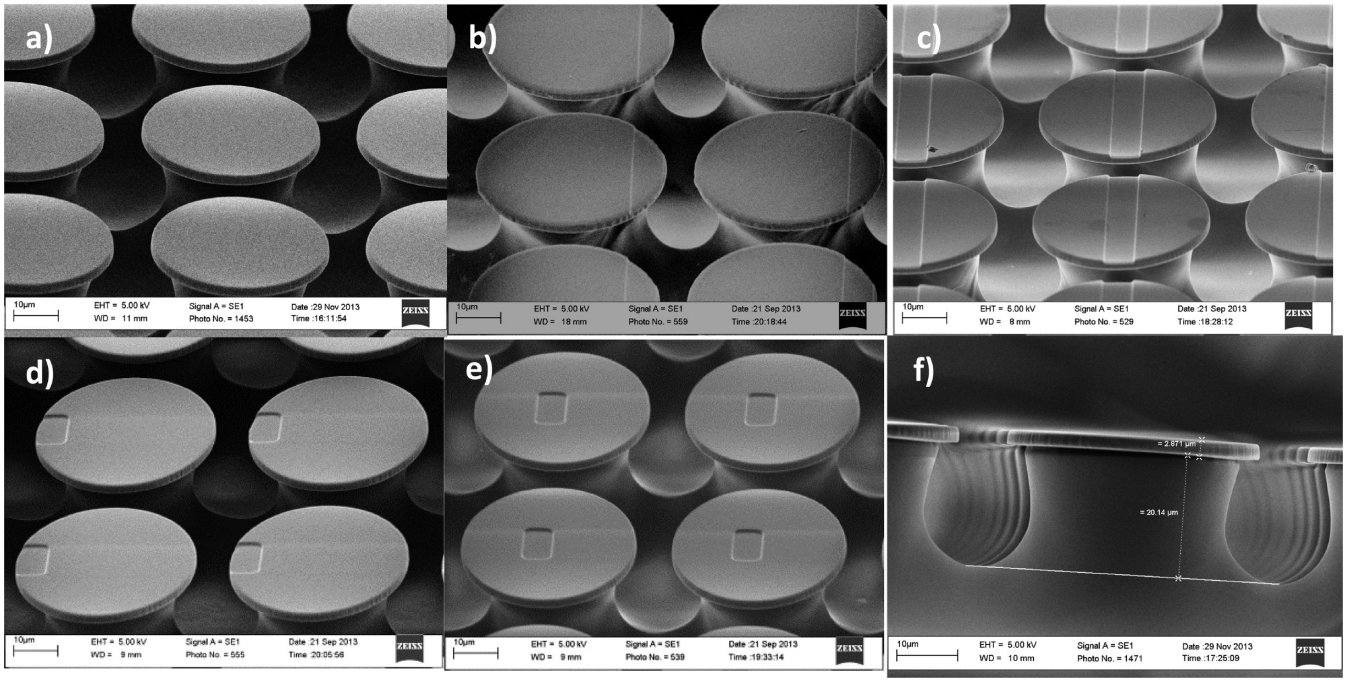

Figure 4. Scanning electron micrographs of gold-coated polystyrene replicas of dry adhesive fibers tested in this work. (a) Isotropic (C_1) samples, (b) C_2 anisotropic bar defect sample, (c) C_3 central bar defect, (d) C_4 anisotropic rectangular defect, (e) C_5 central rectangular defect, and (f) side view of the hourglass shape of fibers with overhanging caps.

temperature for ST-1060 in the literature that we can find, but in the case of SEBS, the lower of the two distinct T_g values is that of the ethylene-butylene and is typically listed as approximately −42 °C on company datatsheets[45] or even lower in specific instances.[46] Our measurements occurred at 22 ± 1 °C and would likely be outside the temperature range found to be significant in the work of Lakhera et al.[44]

The Kraton G1657 and G1645 come in the form of pellets, slightly dusted to prevent sticking. A number of pellets were placed together on a microscope glass slide (Figure 3a) on a hot plate at 200 °C and squeezed to form a single melt (Figure 3b). The silicone master was placed on top of the melt at the desired location. This separate silicone mold was never used for polyurethane to prevent any undesirable contamination or toxic breakdown of polyurethanes. On top of the master and aligned with the Kraton melt, another preheated glass slide was placed and a cylindrical iron mass (∼5 kg) was used as a load to squeeze the melt into the mold to form the mushroom shaped fibers (Figure 3c). The load was left on for 1 min to allow for complete filling and removed afterward. The glass/Kraton/silicone was then removed from the hotplate and placed on a metal surface at room temperature to cool down. The silicone master was then peeled off the Kraton, leaving the thermoplastic adhesives on the bottom glass slide. The Kraton backing layer had low adhesion to the glass and could also be peeled off if desired (Figure 3d).

The fibers fabricated here were mushroom shaped with circular caps of 40 μm diameter and 2.8 μm thickness. The cap overhang was ∼3.2 μm and the fibers were approximately 20 μm tall. Both isotropic and anisotropic mushroom shaped fibers were made using polyurethane and two versions of Kraton thermoplastics. The anisotropic fibers were produced based on a concept and technique described in ref 43, i.e., placement of a defect deliberately at the edge of the cap surface, as shown in Figure 4(b,d, makes the adhesion of the fibers directional. Two different defect shapes, rectangular (C_4, Figure 4d) and bar-like(C_2, Figure 4b), are investigated in this report. In addition, caps with central defects (Figure 4c,e), which is the worst case scenario for mushroom shaped fibers,[37] were also fabricated to compare the vulnerability to defects for each materials. The defects were 800 nm deep for all cases, ∼6 μm wide for C_2 and C_4, and ∼7 μm wide for C_3 and C_5. Due to SEM imaging difficulties of the Kraton polymers directly (due to the overhanging caps curling up after gold deposition from the stress mismatch), the images in Figure 4 are of polystyrene replicas of the fibers, produced using identical times, temperatures, and weights as the Kraton samples. Optical images revealed no significant dimensional differences between these and the Kraton versions, so these are used to demonstrate the basic fiber shapes.

3.2. Adhesion Test. The normal adhesion strength of the fibers was measured using a load-drag-pull test system described elsewhere.[43] The system consists of a 6 mm hemispherical sapphire indenter, attached to a load cell (GSO-25, Transducer Techniques) and moved by means of linear stages. During each trial, a targeted preload of 1 mN was applied followed by dragging a prescribed distance to shear the caps, and pulling off vertically at the same speed (5 μm/s). The load cell determines the maximum force during pull-off, and the preload and pull-off event was recorded by custom software written in LabView. The results are plotted in Figure 5.

From Figure 5a, it can be observed that Kraton G1645 isotropic adhesives performed better than that of Kraton G1657 or ST-1060 polyurethane. Interestingly, the G1645 fibers did not show any significant decline in the adhesion up to a 15 μm shear displacement in either direction, which is not very common for isotropic adhesives, whereas Kraton G1657 and ST-1060 showed a more noticeable decline in adhesion when sheared to either side. It is possible that the softer backing layer aided in reducing the shear sensitivity in this case because if it

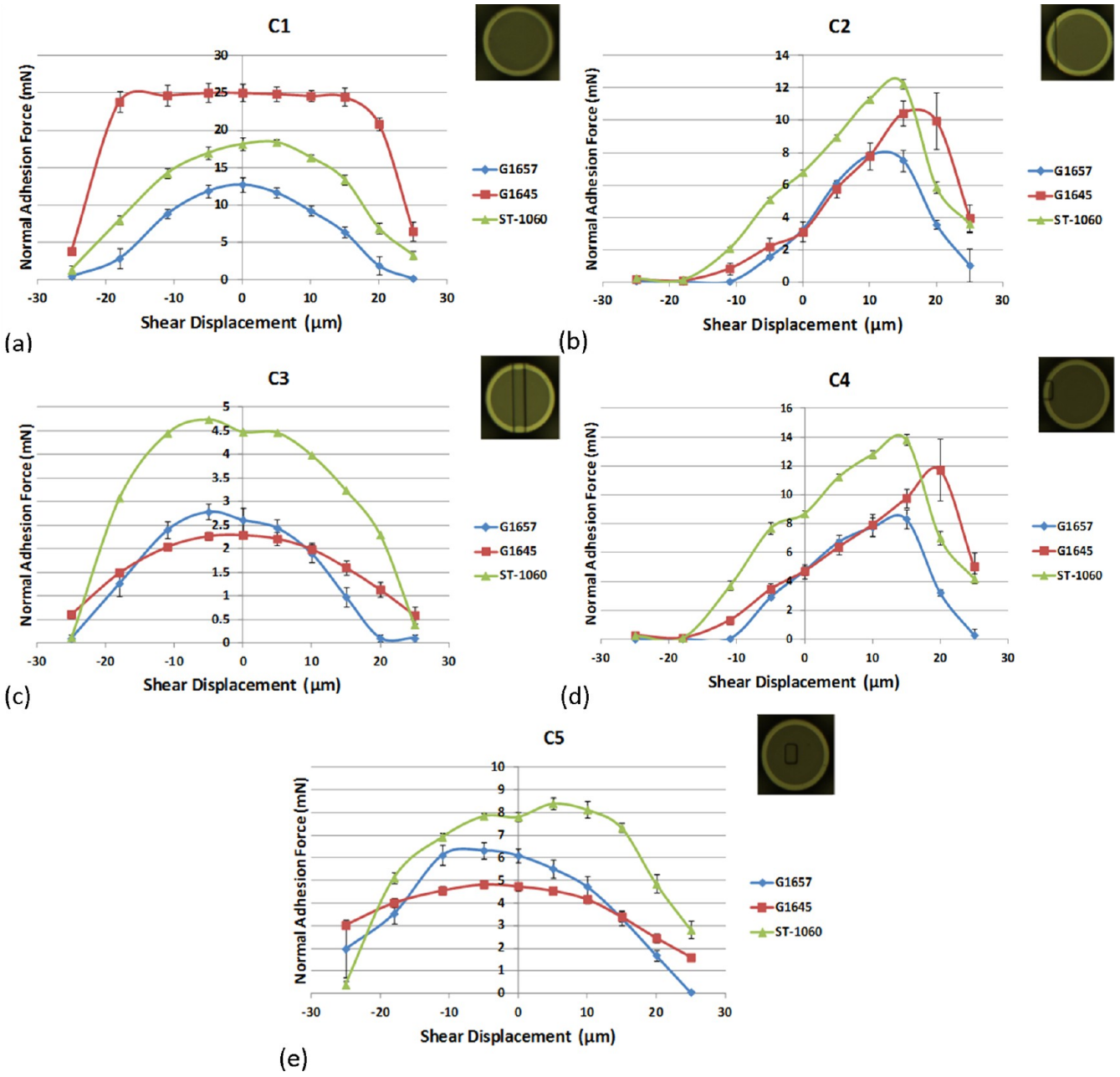

Figure 5. Comparison of load-drag-pull test results for the isotropic fibers (a), anisotropic fibers (b) and (d), and fibers with central cap defects (c and e).

shifted over, there would be lower stress concentrations in the fibers themselves. In the case of the directional fibers, for bar-like defects (C_2 in Figure 5b) and rectangular defects (C_4 in Figure 5d), ST-1060 fibers displayed the greatest maximum adhesion, trailed closely by the G1645 fibers. As expected, the caps with rectangular edge defects (C_4) showed stronger adhesion than the caps with bar-like defects (C_2) for all structural materials. The area of the noncontacting defect surface is less for the rectangular defects as compared to the bar-like defects, resulting in more contact area and consequently stronger adhesion. Kraton G1657 fibers showed the least adhesion in both cases.

The Kraton G1645 fibers seemed to be more susceptible to cap defects, shown by a greater decline in the maximum adhesion strength in the presence of a defect(~80% reduction in adhesion from C_1 to C_5, as compared to ~55% reduction for ST 1060 and ~50% reduction for G1657).

Figure 6 shows the consecutive preload and pull-off events for the polyurethane and Kraton adhesives (C_2 version) at a shear displacement of 10 μm away from the defect (in the "strong" direction). Despite yielding smaller maximum adhesion for a given preload/drag distance, the thermoplastic elastomers would often show much greater tenacity for individual fibers than ST-1060, resulting in longer pull-off events with stepped detachments. These effects were particularly more pronounced for the G1645 samples. The area under the pull-off graph, in Figure 6, for Kraton G1645 is much larger than that of ST-1060, which implies that the effective adhesion energy or work of adhesion is higher, even though the maximum pull-off force is slightly lower for Kraton G1645 as compared to ST-1060. This demonstrates that

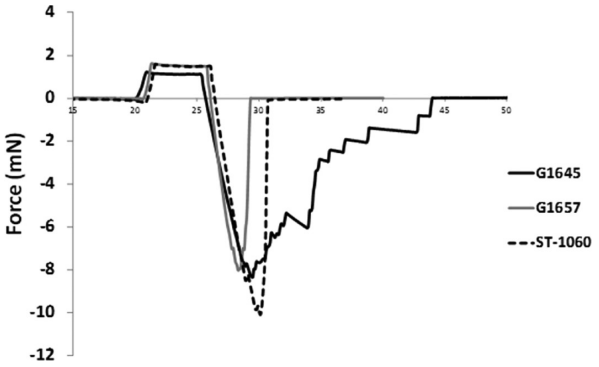

Figure 6. Preload (+ve force) and pull-off (−ve force) vs time for single trials of directional adhesives at a shear displacement of 10 μm away from the defect.

despite slightly inferior performance, these thermoplastic elastomers may have use as a replacement for thermoset materials in less demanding dry adhesive applications.

One aspect of these materials that will be vital for understanding their long-term performance is how much the adhesion may change over time. Many other investigations into this phenomenon have shown that pristine samples will frequently lose a large portion of their initial adhesion strength with repeated preloads.[50−52] Many times, this is attributed to fiber collapse, fiber contamination (via dirt/dust), or oligomer transfer. For our trials, fiber collapse is much less of an issue due to the low aspect ratio, dust is minimal in the test environment, and oligomers are unlikely to transfer given our results in section 2.

The C_2 versions of the Kraton and polyurethane adhesives were tested for 500 cycles with three different shear displacements corresponding to minimum adhesion, adhesion at zero shear, and maximum adhesion in order to determine and compare the useful life cycle of the adhesives. Trials were cycled with 50 displacements at each shear distance (to produce a high, medium, and low adhesion force) and repeated 10 times. These show that multiple displacements in a single direction can influence the subsequent behavior of trials in the opposite direction if enough elongation or plastic deformation occurs. There was approximately 1 min of time between each data point. The results are plotted in Figure 7. The Kraton G1657 showed less stable adhesion behavior immediately after shear displacements change direction.

In the case of the ST-1060 and the G1645, there is a noticeable repeating pattern every 50 cycles in Figure 7a−c, which was the number the test system was setup to do before repeating. The cause is likely some plastic deformation of the fibers in a specific direction, which then gets reversed over several cycles once the shear displacement is reversed. Given that the adhesion tests were all designed to be the exact same location, then the likelihood of any particulate contamination, or tests on defective areas, are mostly ruled out as the cause of the variable adhesion. The G1657 adhesive shows the most variation across the trials, with first an increase and then a decrease in the strongest pull direction during the cyclic loading in Figure 7b. It was also the only sample that significantly changed adhesion in pure normal loads and in the weak direction, so the hypothesis on this one was that the position of the fibers may have been altered through more severe plastic deformation as the trials continued or altered material properties, resulting in very different adhesion values for all

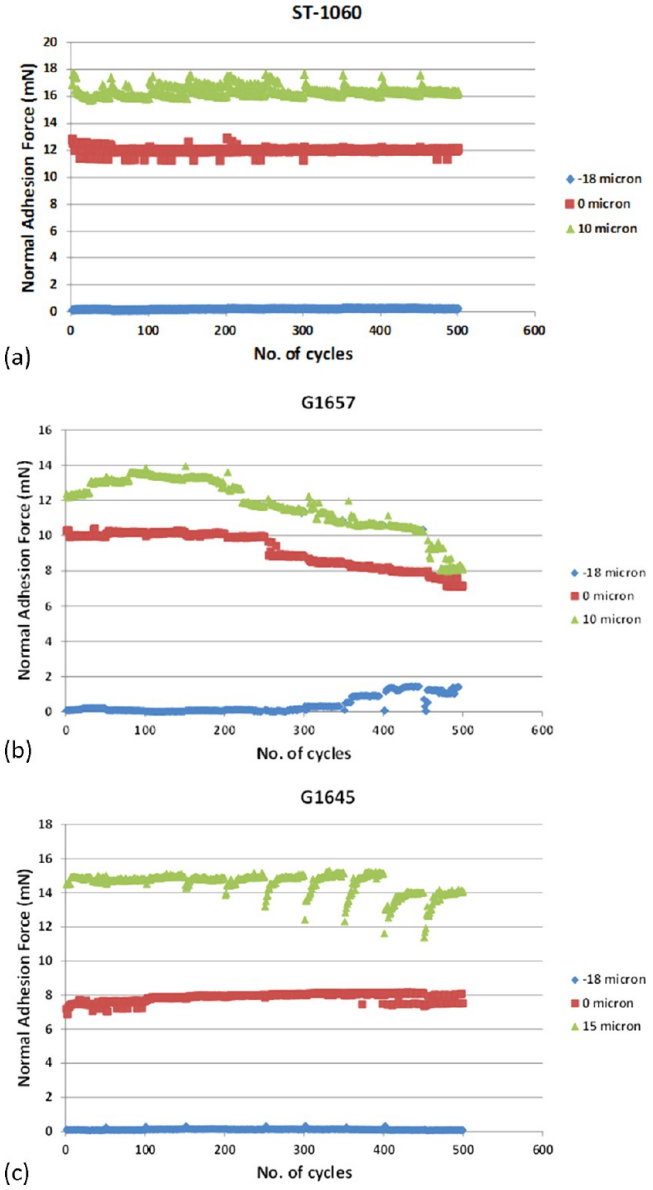

Figure 7. Comparison of the durability of the Kraton and polyurethane adhesives: (a−c) durability tests with 10 cycles of 50 high-medium-low adhesion trials.

levels of shear displacement. For all materials, if shearing in a single direction is consistent, performance rapidly reaches a plateau and we no longer see the cycle dependent performance. Fortunately, as thermoplastic elastomers, G1657 and G1645 may be blended to provide an excellent mix of material properties in future, or compounded with fillers to provide even better material performance. On the basis of the raw resins, however, the G1645 seems to be the superior choice for long-term use.

4. CONCLUSION

We demonstrate for the first time how the thermoplastic elastomer SEBS can successfully be used as an alternative to conventional thermoset elastomers like PDMS and polyurethane for the fabrication of mushroom shaped dry adhesives. Surface contamination tests using X-ray photoelectron spectroscopy (XPS) reveal that although both PDMS and polyurethane transfer traceable amounts of loose oligomers

due to contact, Kraton thermoplastic did not show any significant detectable transfer of its own oligomer, if any. A simple and scalable compression molding system was used to fabricate mushroom shaped fibers directly from a silicone rubber mold in a few minutes, rather than hours. Two variations of thermoplastic elastomer dry adhesives were compared with a thermoset polyurethane counterpart, with one of them showing comparable or better performance in both isotropic and anisotropic performance. With the advantage of faster processing time, lower base material cost, insignificant oligomer transfer, and scalability, the thermocompression molding of thermoplastic elastomers is a viable alternative for the mass production of these mushroom shaped dry adhesives.

AUTHOR INFORMATION

Corresponding Author

*W. B. Khaled. E-mail: wkhaled@ualberta.ca.

Notes

The authors declare no competing financial interest.

ACKNOWLEDGMENTS

The authors thank their lab colleagues Abdul Wasay and Ben Bschaden for their suggestions and technical assistance, and thank the Natural Science and Engineering Research Council of Canada (NSERC) and Micralyne Inc. for their funding of this project under the strategic grants program.

REFERENCES

(1) Autumn, K.; Sitti, M.; Liang, Y. A.; Peattie, A. M.; Hansen, W. R.; Sponberg, S.; Kenny, T. W.; Fearing, R.; Israelachvili, J. N.; Full, R. J. Evidence for van der Waals Adhesion in Gecko Setae. *Proc. Natl. Acad. Sci. U. S. A.* **2002**, *99*, 12252−12256.

(2) Kwak, J.; Kim, T. A Review of Adhesion and Friction Models for Gecko Feet. *Int. J. Precis. Eng. Manuf.* **2010**, *11*, 171−186.

(3) Autumn, K.; Dittmore, A.; Santos, D.; Spenko, M.; Cutkosky, M. Frictional Adhesion: A New Angle on Gecko Attachment. *J. Exp. Biol.* **2006**, *209*, 3569−3579.

(4) Gao, H.; Wang, X.; Yao, H.; Gorb, S.; Arzt, E. Mechanics of Hierarchical Adhesion Structures of Geckos. *Mech. Mater.* **2005**, *37*, 275−285.

(5) Yao, H.; Gao, H. Mechanical Principles of Robust and Releasable Adhesion of Gecko. *J. Adhes. Sci. Technol.* **2007**, *21*, 1185−1212.

(6) Sameoto, D.; Menon, C. Recent Advances in the Fabrication and Adhesion Testing of Biomimetic Dry Adhesives. *Smart Mater. Struct.* **2010**, *19*, 103001.

(7) Kwak, M. K.; Jeong, H. E.; Bae, W. G.; Jung, H.; Suh, K. Y. Anisotropic Adhesion Properties of Triangular-Tip-Shaped Micropillars. *Small* **2011**, *7*, 2296−2300.

(8) Sameoto, D.; Menon, C. Direct Molding of Dry Adhesives with Anisotropic Peel Strength using an Offset Lift-Off Photoresist Mold. *J. Micromech. Microeng.* **2009**, *19*, 115026.

(9) Kim, S.; Sitti, M. Biologically Inspired Polymer Microfibers with Spatulate Tips as Repeatable Fibrillar Adhesives. *Appl. Phys. Lett.* **2006**, *89*, 261911.

(10) Sameoto, D.; Ferguson, B. Robust Large-area Synthetic Dry Adhesives. *J. Adhes. Sci. Technol.* **2012**, *28*, 1−17.

(11) Sameoto, D.; Sharif, H.; Díaz Téllez, J. P.; Ferguson, B.; Menon, C. Nonangled Anisotropic Elastomeric Dry Adhesives with Tailorable Normal Adhesion Strength and High Directionality. *J. Adhes. Sci. Technol.* **2012**, 1−13.

(12) Ferguson, B. J. Improved Gecko Inspired Dry Adhesives Applied to the Packaging of MEMS. MSc Thesis, University of Alberta: Edmonton, Canada, 2013.

(13) Menguc, Y.; Yang, S. Y.; Kim, S.; Rogers, J. A.; Sitti, M. Gecko-Inspired Controllable Adhesive Structures Applied to Micromanipulation. *Adv. Funct. Mater.* **2012**, *22*, 1246−1254.

(14) Carlson, A.; Kim-Lee, H.; Wu, J.; Elvikis, P.; Cheng, H.; Kovalsky, A.; Elgan, S.; Yu, Q.; Ferreira, P. M.; Huang, Y.; Turner, K. T.; Rogers, J. A. Shear-enhanced Adhesiveless Transfer Printing for use in Deterministic Materials Assembly. *Appl. Phys. Lett.* **2011**, *98*.

(15) Yang, S. Y.; Carlson, A.; Cheng, H.; Yu, Q.; Ahmed, N.; Wu, J.; Kim, S.; Sitti, M.; Ferreira, P. M.; Huang, Y.; Rogers, J. A. Elastomer Surfaces with Directionally Dependent Adhesion Strength and their use in Transfer Printing with Continuous Roll-to-Roll Applications. *Adv. Mater.* **2012**, *24*, 2117−2122.

(16) Sharpe, R. B. A.; Burdinski, D.; Van Marel, C. D.; Jansen, J. A. J.; Huskens, J.; Zandvliet, H. J. W.; Reinhoudt, D. N.; Poelsema, B. Ink Dependence of Poly(dimethylsiloxane) Contamination in Microcontact Printing. *Langmuir* **2006**, *22*, 5945−5951.

(17) Yang, L.; Shirahata, N.; Saini, G.; Zhang, F.; Pei, L.; Asplund, M. C.; Kurth, D. G.; Ariga, K.; Sautter, K.; Nakanishi, T.; Smentkowski, V.; Linford, M. R. Effect of Surface Free Energy on PDMS Transfer in Microcontact Printing and its Application to ToF-SIMS to Probe Surface Energies. *Langmuir* **2009**, *25*, 5674−5683.

(18) Yunus, S.; De Crombrugghe, D. L.; Poleunis, C.; Delcorte, A. Diffusion of Oligomers from Polydimethylsiloxane Stamps in Microcontact Printing: Surface Analysis and Possible Application. *Surf. Interface Anal.* **2007**, *39*, 922−925.

(19) Glasmastar, K.; Gold, J.; Andersson, A.; Sutherland, D. S.; Kasemo, B. Silicone Transfer during Microcontact Printing. *Langmuir* **2003**, *19*, 5475−5483.

(20) Graham, D. J.; Price, D. D.; Ratner, B. D. Solution Assembled and Microcontact Printed Monolayers of Dodecanethiol on Gold: A Multivariate Exploration of Chemistry and Contamination. *Langmuir* **2002**, *18*, 1518−1527.

(21) Böhm, I.; Lampert, A.; Buck, M.; Eisert, F.; Grunze, M. A Spectroscopic Study of Thiol Layers Prepared by Contact Printing. *Appl. Surf. Sci.* **1999**, *141*, 237−243.

(22) Zhou, Y.; Valiokas, R.; Liedberg, B. Structural Characterization of Microcontact Printed Arrays of Hexa(ethylene glycol)-Terminated Alkanethiols on Gold. *Langmuir* **2004**, *20*, 6206−6215.

(23) Langowski, B. A.; Uhrich, K. E. Oxygen Plasma-Treatment Effects on Si Transfer. *Langmuir* **2005**, *21*, 6366−6372.

(24) Thomson, N. R.; Bower, C. L.; McComb, D. W. Identification of Mechanisms Competing with Self-Assembly during Directed Colloidal Deposition. *J. Mater. Chem.* **2008**, *18*, 2500−2505.

(25) Perl, A.; Péter, M.; Ravoo, B. J.; Reinhoudt, D. N.; Huskens, J. Heavyweight Dendritic Inks for Positive Microcontact Printing. *Langmuir* **2006**, *22*, 7568−7573.

(26) Zhao, Y.; Li, M.; Lu, Q.; Shi, Z. Superhydrophobic Polyimide Films with a Hierarchical Topography: Combined Replica Molding and Layer-by-Layer Assembly. *Langmuir* **2008**, *24*, 12651−12657.

(27) Trimbach, D.; Stapert, H.; van Orselen, J.; Jandt, K.; Bastiaansen, C.; Broer, D. Improved Microcontact Printing of Proteins using Hydrophilic Thermoplastic Elastomers as Stamp Materials. *Adv. Eng. Mater.* **2007**, *9*, 1123−1128.

(28) Ranade, M. B. Adhesion and Removal of Fine Particles on Surfaces. *Aerosol Sci. Technol.* **1987**, *7*, 161−176.

(29) Wigenius, J. A.; Hamedi, M.; Inganäs, O. Limits to Nanopatterning of Fluids on Surfaces in Soft Lithography. *Adv. Funct. Mater.* **2008**, *18*, 2563−2571.

(30) Briseno, A. L.; Roberts, M.; Ling, M.; Moon, H.; Nemanick, E. J.; Bao, Z. Patterning Organic Semiconductors Using Dry Poly(dimethylsiloxane) Elastomeric Stamps for Thin Film Transistors. *J. Am. Chem. Soc.* **2006**, *128*, 3880−3881.

(31) Yang, Z.; Belu, A. M.; Liebmann-Vinson, A.; Sugg, H.; Chilkoti, A. Molecular Imaging of a Micropatterned Biological Ligand on an Activated Polymer Surface. *Langmuir* **2000**, *16*, 7482−7492.

(32) Wang, X.; Östblom, M.; Johansson, T.; Inganäs, O. PEDOT Surface Energy Pattern Controls Fluorescent Polymer Deposition by Dewetting. *Thin Solid Films* **2004**, *449*, 125−132.

(33) Iyer, N.; Saka, N. Jung-Hoon Chun Contamination of Silicon Surface due to Contact with Solid Polymers. *IEEE Trans. Semicond. Manuf.* **2001**, *14*, 85−96.

(34) Reddy, S.; Arzt, E.; del Campo, A. Bioinspired Surfaces with Switchable Adhesion. *Adv. Mater.* **2007**, *19*, 3833−3837.
(35) Majidi, C.; Groff, R. E.; Maeno, Y.; Schubert, B.; Baek, S.; Bush, B.; Maboudian, R.; Gravish, N.; Wilkinson, M.; Autumn, K.; Fearing, R. S. High Friction from a Stiff Polymer using Microfiber Arrays. *Phys. Rev. Lett.* **2006**, *97*.
(36) Lee, J.; Majidi, C.; Schubert, B.; Fearing, R. S. Sliding-induced Adhesion of Stiff Polymer Microfibre Arrays. I. Macroscale Behaviour. *J. R. Soc., Interface* **2008**, *5*, 835−844.
(37) Carbone, G.; Pierro, E.; Gorb, S. N. Origin of the Superior Adhesive Performance of Mushroom-Shaped Microstructured Surfaces. *Soft Matter* **2011**, *7*, 5545−5552.
(38) Spuskanyuk, A. V.; McMeeking, R. M.; Deshpande, V. S.; Arzt, E. The Effect of Shape on the Adhesion of Fibrillar Surfaces. *Acta Biomater.* **2008**, *4*, 1669−1676.
(39) Kim, S.; Cheung, E.; Sitti, M. Wet Self-Cleaning of Biologically Inspired Elastomer Mushroom Shaped Microfibrillar Adhesives. *Langmuir* **2009**, *25*, 7196−7199.
(40) Murphy, M. P.; Aksak, B.; Sitti, M. Gecko-Inspired Directional and Controllable Adhesion. *Small* **2009**, *5*, 170−175.
(41) Bartlett, M. D.; Croll, A. B.; King, D. R.; Paret, B. M.; Irschick, D. J.; Crosby, A. J. Looking Beyond Fibrillar Features to Scale Gecko-Like Adhesion. *Adv. Mater.* **2012**, *24*, 1078−1083.
(42) Nanolab Technologies. XPS Binding Energies (BE) and Scofield's Relative Sensitivity Factor (RSF) Chart. Available at: http://www.nanolabtechnologies.com/pdf/Scofield-Table-of-BEs-and-RSFs.pdf (accessed March 23, 2014).
(43) Khaled, W. B.; Sameoto, D. Anisotropic Dry Adhesive via Cap Defects. *Bioinspiration Biomimetics* **2013**, *8*, 044002.
(44) Lakhera, N.; Graucob, A.; Schneider, A. S.; Kroner, E.; Arzt, E.; Yakacki, C. M.; Frick, C. P. Effect of Viscoelasticity on the Spherical and Flat Adhesion Characteristics of Photopolymerizable Acrylate Polymer Networks. *Int. J. Adhes. Adhes.* **2013**, *44*, 184−194.
(45) Kraton Polymers. Kraton Polymers Brochure. Available at: http://docs.kraton.com/kraton/attachments/downloads/81311AM.pdf (accessed March 23, 2014).
(46) Roy, E.; Galas, J.; Veres, T. Thermoplastic Elastomers for Microfluidics: Towards a High-Throughput Fabrication Method of Multilayered Microfluidic Devices. *Lab Chip* **2011**, *11*, 3193−3196.
(47) BJB Enterprises, Inc. ST-1060 A/B Data Sheet. Available at: http://www.bjbenterprises.com/pdf/ST-1060.pdf (accessed March 23, 2014).
(48) Kraton Polymers. Kraton G1645 M Polymer Data Sheet. Available at: http://docs.kraton.com/tl_warehouse/pdf_data_docs/WG_4244_WG4F23.tmp.pdf (accessed March 23, 2014).
(49) Kraton Polymers. Kraton G1657 M Polymer Data Sheet. Available at: http://docs.kraton.com/tl_warehouse/pdf_data_docs/WG_4244_WG93AE.tmp.pdf (accessed March 23, 2014).
(50) Kroner, E.; Maboudian, R.; Arzt, E. Adhesion Characteristics of PDMS Surfaces during Repeated Pull-Off Force Measurements. *Adv. Eng. Mater.* **2010**, *12*, 398−404.
(51) Davies, J.; Haq, S.; Hawke, T.; Sargent, J. P. A Practical Approach to the Development of a Synthetic Gecko Tape. *Int. J. Adhes. Adhes.* **2009**, *29*, 380−390.
(52) Murphy, M. P.; Kim, S.; Sitti, M. Enhanced Adhesion by Gecko-Inspired Hierarchical Fibrillar Adhesives. *ACS Appl. Mater. Interfaces* **2009**, *1*, 849−855.